

# Differential Via Modeling Methodology

Lambert Simonovich, *Member, IEEE*, Eric Bogatin *Member, IEEE*, and Yazi Cao, *Member, IEEE*

**Abstract**— The paper describes a novel method of modeling the differential via on multilayered printed circuit boards used in high speed digital designs based on the analytical equations for characteristic impedance and effective dielectric constant. In the absence of measured or EM simulated data traditionally needed to extract these parameters, this method can quickly and efficiently predict the behavior of the differential via holes on printed circuit boards using a circuit simulator.

**Index Terms**— Circuit modeling, Circuit simulation, Via modeling

## I. INTRODUCTION:

PRESENT integrated circuit (IC) technology advancements are facilitating data rates in excess of 10 Gb/s. Printed circuit board (PCB) through hole via parasitics are becoming more of a factor affecting bit error rate (BER) performance. Accurate via modeling for topology simulations are a must and often require sophisticated electro-magnetic (EM) modeling tools.

Behavioral and circuit models are two generic types used to simulate high speed serial links. S-parameters are called behavioral models because they describe the behavior of the structure with respect to incident waveforms from calibrated ports. Behavioral models extracted from EM-field solvers are frequently described by S-parameters.

Measured S-parameter behavioral models extracted from physical structures are limited because they represent everything connected between the calibrated reference planes of the vector network analyzer (VNA). In order to leave behind just the S-parameter's structure of interest, elaborate de-embedding and calibration schemes are needed to remove fixture effects from the measurement. Even then, they only represent one sample of a given construction. It is impossible to perform sensitivity analysis with a single behavior model. Their usefulness lies in model development to help build, calibrate and validate EM or circuit models.

Manuscript received April 14, 2010. This work was supported in part by Lamsim Enterprises Inc., Bogatin Enterprises LLC and Agilent EEsof EDA for supplying the software license to complete this work.

Lambert Simonovich is with Lamsim Enterprises Inc., Stittsville, ON, Canada K2S 0A6 (email: [lsimonovich@lamsimenterprises.com](mailto:lsimonovich@lamsimenterprises.com)).

Eric Bogatin is with Bogatin Enterprises LLC., Olathe, KS, U.S.A. 66061 (e-mail: [eric@BeTheSignal.com](mailto:eric@BeTheSignal.com))

Yazi Cao is with the Department of Electronics, Carleton University, Ottawa, ON, Canada K1S 5B6 (e-mail: [yazi.cao@hotmail.com](mailto:yazi.cao@hotmail.com)).

A circuit model is a schematic representation of a physical structure. There can be more than one circuit that describes it. Each is capable of giving the same performance, up to some bandwidth. When run in a circuit simulator, they predict a measureable performance of the structure and can be parameterized so that worst case, min/max analysis can be explored quickly.

There are cases when quick analysis must be performed to gain an intuitive sense of system performance and assess design trade-offs to guide the final implementation and detailed design analysis. Using traditional EM modeling tools can be a time consuming exercise. They require a high degree of skill and expertise to create a trustworthy model. Once completed there is no way to sanitize the results to ensure it has been built correctly.

Our recent papers, [3], [5], have demonstrated that a simple circuit model for a differential via transition, consisting of two simple, coupled transmission line circuit models, can be used to accurately describe a real differential via to very high bandwidth. In both papers, the measured S-parameters were used to extract the effective dielectric constant ( $D_{keff}$ ) used to calculate the odd-mode impedance for the differential via circuit model. Unfortunately, without EM-field solver or measured S-parameter data, the effective dielectric constant, key to producing an accurate circuit model, was unattainable.

This paper presents a novel equation based methodology to develop a simple circuit model of a defined differential via structure. Analytically derived equations replace the need for measured data or EM simulated results to extract parameters for characteristic impedance and effective dielectric constant used in the model. Correlation to an EM-field solver and measured results are included to demonstrate the merits of this new methodology.

## II. BACKGROUND:

A twin-rod transmission line geometry as illustrated in **Figure 1** is one of three cross-sectional geometries that have exact equations for characteristic impedance. The other two geometries are coaxial and rod-over-plane. All three relationships assume the dielectric material is homogeneous and completely fills the space whenever there are electric fields.

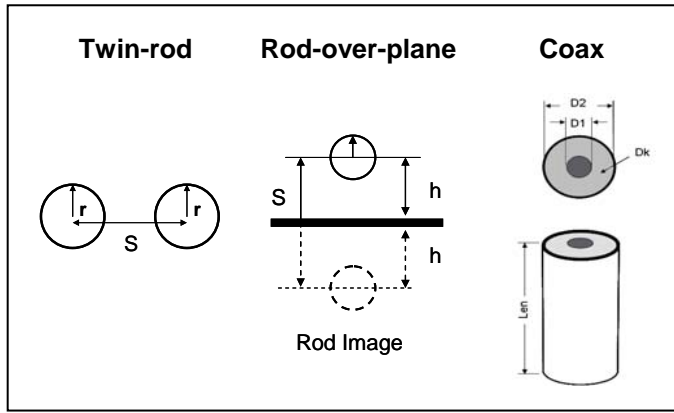


Figure 1 Twin-rod, Rod-over-plane and Coax structures.

The relationships between capacitance, loop inductance and impedance of twin-rod geometry are described by the following equations [2]:

$$C_{twin} = \frac{7.06E-13}{\ln\left(\frac{s}{2r}\left[1 + \sqrt{1 - \left(\frac{2r}{s}\right)^2}\right]}\right)} \times Dk \times Len \quad (1)$$

$$L_{twin} = 10.16E-9 \times \ln\left(\frac{s}{2r} + \sqrt{\left(\frac{s}{2r}\right)^2 - 1}\right) \times Len \quad (2)$$

$$Z_{diff} = \frac{120}{\sqrt{Dk}} \times \ln\left(\frac{s}{2r} + \sqrt{\left(\frac{s}{2r}\right)^2 - 1}\right) \quad (3)$$

Where:

$C_{twin}$  = Capacitance between twin-rods - F

$L_{twin}$  = Inductance between twin-rods - H

$Z_{diff}$  = Differential impedance of twin-rods -  $\Omega$

$Dk$  = Dielectric constant of material

$Len$  = Length of the rods

$r$  = Radius of the rods

$s$  = Space between the rods

When driven differentially, the electro-magnetic fields create a virtual return plane at exactly one half of the spacing between the rods. Each rod therefore behaves like a single rod-over-plane geometry.

The odd-mode capacitance is the capacitance of each rod to virtual return plane and is equal to twice the capacitance between rods.

$$C_{odd} = 2 \times C_{twin} \quad (4)$$

The odd-mode loop inductance is the inductance of each rod to virtual return plane and equal to one half the loop inductance between rods.

$$L_{odd} = \frac{L_{twin}}{2} \quad (5)$$

The odd-mode impedance of each rod is half of the differential impedance, and is equivalent to the rod-over-plane impedance.

$$Z_{odd} = \frac{Z_{twin}}{2} \quad (6)$$

The coaxial transmission line geometry consists of a center conductor imbedded within dielectric material and surrounded by a continuous shield

The relationships between capacitance, loop inductance and impedance of coaxial geometries are [2]:

$$C_{coax} = \frac{1.41E-12}{\ln\left(\frac{D2}{D1}\right)} Dk \times Len \quad (7)$$

$$L_{coax} = 5.08E-9 \times \ln\left(\frac{D2}{D1}\right) \times Len \quad (8)$$

$$Z_0 = \frac{60}{\sqrt{Dk}} \times \ln\left(\frac{D2}{D1}\right) \quad (9)$$

Where:

$C_{coax}$  = Capacitance - F

$L_{coax}$  = Inductance - H

$Z_0$  = Characteristic Impedance -  $\Omega$

$Dk$  = Dielectric constant

$Len$  = Length of the rods

$D1$  = Diameter of conductor

$D2$  = Diameter of shield

An oval variation of a coaxial structure is a form of an elliptic coaxial structure shown in Figure 2. Gunston [8] derived the relationships between capacitance, loop inductance and impedance of elliptic coaxial geometries as:

$$C_{ellip} \cong \frac{1.41E-12}{\ln\left(\frac{W'+b}{w+t}\right)} \times Dk \times Len \quad (10)$$

$$L_{ellip} \cong 5.08E-9 \times \ln\left(\frac{W'+b}{w+t}\right) \times Len \quad (11)$$

$$Z_0 \cong \frac{60}{\sqrt{Dk}} \times \ln\left(\frac{W'+b}{w+t}\right) \quad (12)$$

Where:

$C_{ellip}$  = Capacitance - F  
 $L_{ellip}$  = Inductance - H  
 $Z_o$  = Characteristic Impedance -  $\Omega$   
 $Dk$  = Dielectric constant  
 $Len$  = Length of the rods  
 $\left(\frac{W'+b}{w+t}\right)$  = Oval dimensions **Figure 2**

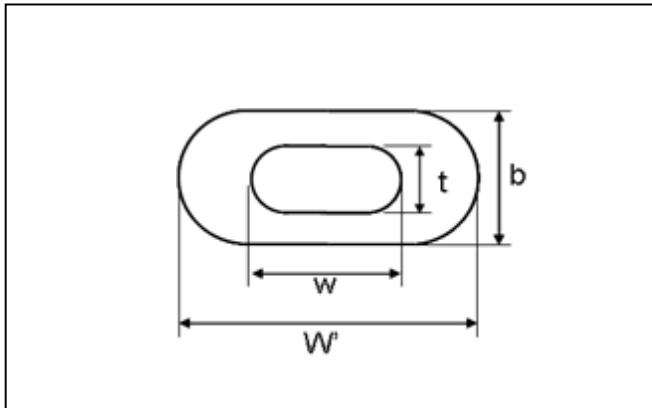


Figure 2 Elliptic (oval) coaxial transmission line structure.

### III. CIRCUIT MODEL:

#### A. Equivalent circuit of differential via:

A simple twin-rod model for a differential via transition, consisting of a uniform differential pair, can be used to describe a differential via using simple coupled transmission lines as illustrated in **Figure 3**. When driven differentially, the odd-mode parameters are of major importance and the even-mode parameters have no impact on differential performance. For modeling convenience, the odd and even-mode parameters were set to the same values. As a result, the odd-mode characteristic impedance ( $Z_{odd}$ ) equals to even-mode characteristic impedance ( $Z_{even}$ ), which cause the coupling coefficient to be equal to zero for a pair of coupled transmission lines. The common impedance is undefined due to its sensitivity on the return vias which cannot be modeled using this methodology.

The secret to this simple circuit model is in using the correct value for  $Dk_{eff}$ . In an earlier paper [3], it was suggested the effective dielectric constant in the x-y axis ( $Dk_{xy}$ ) was predominated by the glass fiber density surrounding the via hole structure.

A later paper [5] theorized it could be a combination of the anisotropic properties of the dielectric material plus the capacitive loading effect of the anti-pads thereby lowering the overall odd-mode via impedance and raising the effective  $Dk$ . Unfortunately it was not possible to prove this before publication.

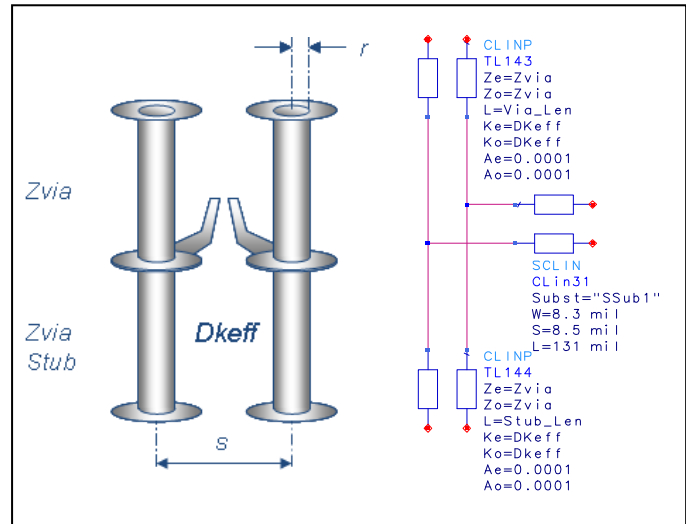


Figure 3 Agilent ADS circuit based twin-rod via model.

In a subsequent paper [7], the dielectric material was shown to have a  $Dk$  anisotropic factor approximately 18% higher in the x-y axis (4.30) over the average the z-axis (3.64). This corroborates well with Dankov et al's work [4] showing glass reinforced laminates have an anisotropic factor between 15-20%.

#### B. Developing analytical equations for $Z_{odd}$ and $Dk_{eff}$ :

Consider the differential via structure illustrated in **Figure 4**. When there are many copper layers in the PCB stack-up, it resembles two coaxial transmission lines where the shield is created by the oval anti-pads of the reference layers. The thinner the dielectric between these layers, the more it behaves like a coaxial structure from an electrostatic point of view. For PCB stack-ups with fewer copper layers and thick dielectric between planes, the differential via behave more like a twin-rod structure from an electrostatic perspective. When there are many copper layers, the odd-mode via capacitance can therefore be estimated using the following formula based on elliptical coaxial transmission line model (**Figure 2**):

$$C_{via} = C_{ellip} \cong \frac{1.41E-12}{\ln\left(\frac{W'+b}{w+t}\right)} \times Dk_{avg} \times Len \quad (13)$$

From a magnetostatic point of view, the via structure behaves more like a twin-rod transmission line because the magnetic field lines are not contained by a continuous shield throughout the via length. For that reason, odd-mode via loop inductance can be estimated by the following equation:

$$L_{via} = \frac{L_{twin}}{2} = 5.08E-9 \times \ln \left( \frac{s}{2r} + \sqrt{\left(\frac{s}{2r}\right)^2 - 1} \right) \times Len \quad (14)$$

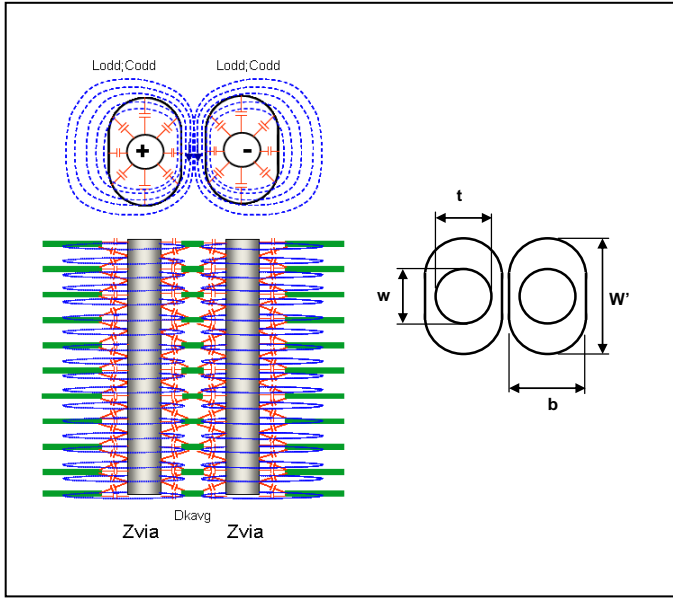


Figure 4 EM Field relationship illustration of twin-rod via model with oval anti-pads. The blue magnetic flux rings represent the odd-mode inductance while the red capacitors represent the electric field from via barrels to oval anti-pads.

Knowing the odd-mode via inductance and capacitance, the odd-mode via impedance can be approximated by [11]:

$$Z_{odd} = Z_{via} \cong \frac{60}{\sqrt{Dk_{avg}}} \times \ln \left( \frac{s}{2r} + \sqrt{\left(\frac{s}{2r}\right)^2 - 1} \right) \times \ln \left( \frac{W'+b}{w+t} \right) \quad (15)$$

Where:

- $L_{via}$  = Odd-mode via inductance - H
- $C_{via}$  = Odd-mode via capacitance - F
- $Z_{via}$  = Odd-mode via impedance -  $\Omega$
- $s$  = via to via pitch
- $r$  = radius of via barrel = Drill diameter

$$Dk_{avg} = \frac{(Dk_{xy} + Dk_z)}{2}$$

The bulk dielectric constant  $Dk_{avg}$  is due to the combination of resin and glass weave distribution. If a differential signal is propagated between the twin rods, it would see this bulk dielectric constant. However, it also sees the capacitive loading from the fringe fields between the barrel and the planes it passes through. This distributed capacitance effectively lowers the odd-mode impedance of the via and increases the effective dielectric constant.

The effective dielectric constant can be evaluated based on

how much the via's odd-mode impedance is decreased. Based on the twin rod formula, the via's odd-mode impedance can be expressed as follows:

$$Z_{via} = \frac{Z_{twin}}{2} \cong \frac{60}{\sqrt{Dk_{eff}}} \times \ln \left( \frac{s}{2r} + \sqrt{\left(\frac{s}{2r}\right)^2 - 1} \right)$$

Substituting the odd-mode impedance from equation (15) into the equation above, and solving for  $Dk_{eff}$  yields [11]:

$$Dk_{eff} = \left[ \frac{60}{Z_{via}} \times \ln \left( \frac{s}{2r} + \sqrt{\left(\frac{s}{2r}\right)^2 - 1} \right) \right]^2$$

$$Dk_{eff} = Dk_{avg} \times \frac{\ln \left( \frac{s}{2r} + \sqrt{\left(\frac{s}{2r}\right)^2 - 1} \right)}{\ln \left( \frac{W'+b}{w+t} \right)} \quad (16)$$

### C. HFSS vs. analytical correlation for $Dk_{eff}$ :

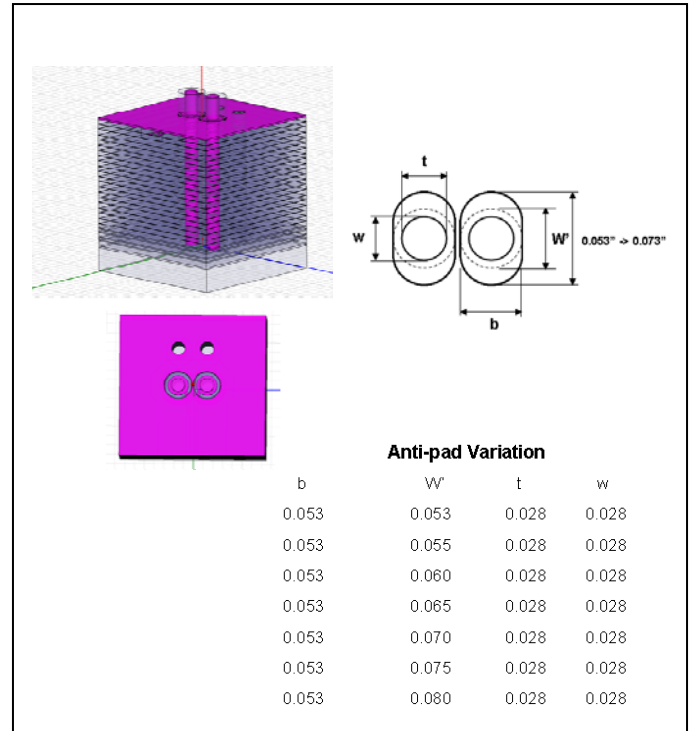


Figure 5 Ansoft HFSS model oval anti-pad variation.  $Dk=1$

The HFSS [9] model shown in Figure 5 developed for [7] was reused to validate the circuit model against  $Dk_{eff}$ . The anti-pad dimension ( $W'$ ) was varied in length according to the table. A  $Dk = 1$  was used to simplify the analysis and remove any dielectric anisotropic ambiguity.

For each anti-pad dimension equation (16) was used to calculate  $D_{keff}$ .

By extracting the  $\frac{1}{4}$ -wave resonant frequency  $f_0$  from the HFSS simulations,  $D_{keff}$  was calculated using the following equation [3]:

$$D_{keff} = \left[ \frac{c}{4 * Stub\_length * f_0} \right]^2 \tag{17}$$

$c$  = speed of light = 2.99E+8 m/s (1.18E+10 in/s)  
 $f_0$  =  $\frac{1}{4}$  wave resonant frequency  
 $Stub\_len$  = Stub length

The results are presented in Table 1 and plotted in Figure 6. They show excellent correlation to HFSS field solver results with better than 1% accuracy for oval anti-pad length to width ratios of less than 1.2:1, and 5% for 1.5:1 ratio.

Table 1  
 Comparison of  $D_{keff}$  calculated vs HFSS 3D field solver for  $D_k=1$ .  
 Metric conversion:  $0.001'' = 25.4\mu m$

Stub_Len inch	A-pad_W inch	A-pad_L inch	Res Freq HFSS Sim Hz	$D_{keff\_Sim}$ HFSS	$D_{keff\_Cal}$ Formula	Delta %	Zodd Cal ohms
0.264	0.053	0.053	7.63E+09	2.15	2.16	0.5%	56.2
0.264	0.053	0.055	7.75E+09	2.08	2.10	0.8%	57.1
0.264	0.053	0.060	7.98E+09	1.96	1.96	-0.1%	59.0
0.264	0.053	0.065	8.19E+09	1.86	1.85	-0.8%	60.8
0.264	0.053	0.070	8.33E+09	1.80	1.75	-2.8%	62.4
0.264	0.053	0.075	8.43E+09	1.76	1.67	-5.3%	64.0
0.264	0.053	0.080	8.52E+09	1.72	1.59	-7.5%	65.5

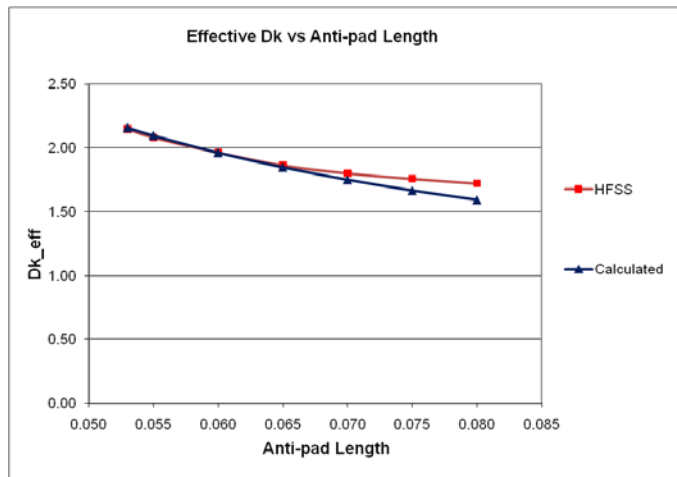


Figure 6 Comparison of  $D_{keff}$  calculated vs HFSS 3D field solver simulation for  $D_k=1$

D. Investigating the stub portion of a differential via test structure:

A 26 layer test vehicle was designed and fabricated [3], [5], [7]. There were 10 internal stripline layers, 12 reference layers and 4 dedicated power layers. Each differential pair had a nominal line width of 8 mils (203  $\mu m$ ) with 9 mil (2229  $\mu m$ ) space and was 6 inches (15.24 cm) long. Half ounce copper was used for the internal layers. The dielectric material was N4000-13. The total dielectric spacing between the reference planes was nominally 21.7 mils (551  $\mu m$ ). Cores were 10 mils (254  $\mu m$ ), while 11 mil (279  $\mu m$ ) prepreg consisted of 2 x 1080 plus 1 x 2116 style sheets. The finished differential pair impedance was targeted for 100 ohms +/- 10 percent. Each pair was terminated at each end with 2 x 24 mil (610  $\mu m$ ) finished hole size (FHS) vias. The intra-pair via pitch was 59 mils (1.5 mm). There were 2 adjacent ground vias; 79 mils (2.0 mm) away for each respective signal via. A typical stub portion of the differential via of the test structure is illustrated in Figure 7. In the actual PCB stack-up, the reference plane layers have oval anti-pads, while the signal layers have copper plane-fill with round anti-pads.

The stub region has two different cross sections, labeled as Stub1 and Stub2. Throughout Stub1 thickness, the anti-pads alternate between round and oval. The Stub2 thickness represents the power plane layers with thinner dielectric between planes and thicker copper layers.

The cross-section includes the electric and magnetic field distributions between the via barrels and the clearance holes in the planes. The electric field lines through Stub1 will spread onto the cavities between reference planes to roughly the extent of the round anti-pad diameter as shown except for the thickness of the oval anti-pad copper layers where the electric field will be contained to the oval dimension. To simplify analysis, these layers are subtracted from Stub1's overall thickness and added to Stub2's thickness because they will have the same properties.

Given that fringe field via capacitance loading in the Stub1 region will be lower than in the Stub2 region, the speed of propagation in the Stub1 region will be higher than in the Stub2 region. Therefore,  $D_{keff1}$  will be lower than  $D_{keff2}$ .

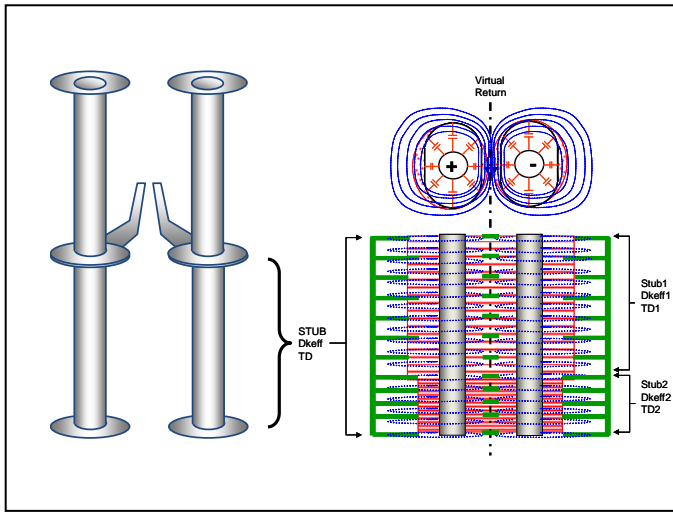


Figure 7 Stub portion of differential via. Oval anti-pads on reference plane layers and round anti-pads on signal layers. The blue magnetic flux rings represent the odd-mode inductance while the red capacitors represent the electric field from via barrels to anti-pads.

Stub resonance happens when a portion of the signal travelling through the active region of a via is diverted down into the stub section. It then reflects off the open-circuited end, and returns later to recombine with the main signal. At some high frequency, if the round trip delay ( $2TD$ ) from the active region of the via to the end of the stub and back equals half of a cycle, the main wave and the reflected wave appear 180 degrees out of phase, producing destructive signal cancellation. That frequency is called the  $\frac{1}{4}$ -wave resonant frequency  $f_o$ . The longer the length of the stub is, the lower the resonant frequency.

effective dielectric constant surrounding the via hole structure changes. The total time delay,  $TD$  is the sum of  $TD1$  and  $TD2$ . This time delay will determine the  $\frac{1}{4}$ -wave frequency notch in the  $S_{21}$  insertion loss plot.

Therefore, the  $\frac{1}{4}$ -wave resonant frequency (Hz) can be expressed as follows:

$$f_o = \frac{1}{4 \times TD} = \frac{1}{4 \times (TD_1 + TD_2)} \quad (18)$$

Where;

$TD_1, TD_2$  = time delay in each stub region

The time delay through each stub region can be calculated from the geometrical length of the region and the effective dielectric constant in each region.

$$TD_1 = \frac{Stub\_len1}{c} \times \sqrt{Dkeff1}$$

$$TD_2 = \frac{Stub\_len2}{c} \times \sqrt{Dkeff2}$$

The effective dielectric constant in each stub region can be calculated based on equation (16) using the different clearance hole geometry of each region.

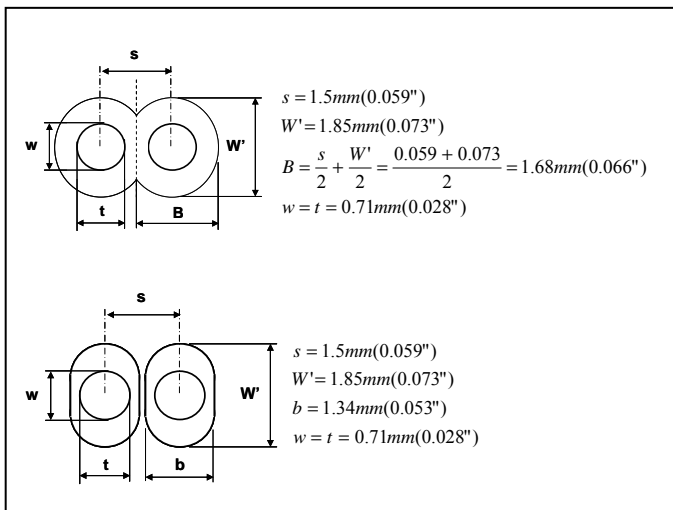


Figure 8 Round vs. oval anti-pad details of the test vehicle.

The specifics of the differential via anti-pads are shown in **Figure 8**. The round anti-pads overlap each other due to the via-via spacing ( $s$ ).

The propagation delay through the stub varies as the

$$Dkeff1 = Dkavg \times \frac{\ln\left(\frac{s}{2r} + \sqrt{\left(\frac{s}{2r}\right)^2 - 1}\right)}{\ln\left(\frac{W'+B}{w+t}\right)}$$

$$Dkeff2 = Dkavg \times \frac{\ln\left(\frac{s}{2r} + \sqrt{\left(\frac{s}{2r}\right)^2 - 1}\right)}{\ln\left(\frac{W'+b}{w+t}\right)}$$

$c$  = speed of light =  $2.99E+8$  m/s ( $1.18E+10$  in/s)

$s$  = via to via pitch

$r$  = radius of via barrel = Drill dia.

$Stub\_len1 + Stub\_len2$  = Stub length

$$Dkavg = \frac{(Dkxy + Dkz)}{2}$$

$\left(\frac{W'+B}{w+t}\right)$  = Round anti-pad dimensions per **Figure 8**



$$\left(\frac{W'+b}{w+t}\right) = \text{Oval anti-pad dimensions per Figure 8}$$

Once the  $\frac{1}{4}$ -wave resonant frequency is calculated, a new  $D_{keff}$  and  $Z_{via}$  approximating the entire stub length can be calculated using the following equations for each anti-pad dimension [3]:

$$D_{keff} = \left[ \frac{c}{4 \times \text{Stub\_length} \times f_0} \right]^2$$

$$Z_{via} \cong \frac{(Z_{via\_Stub1} + Z_{via\_Stub2})}{2}$$

Where;

$$Z_{via\_Stub1} \cong \frac{60}{\sqrt{D_{kavg}}} \times \sqrt{\ln\left(\frac{s}{2r} + \sqrt{\left(\frac{s}{2r}\right)^2 - 1}\right)} \times \ln\left(\frac{W'+B}{w+t}\right)$$

$$Z_{via\_Stub2} \cong \frac{60}{\sqrt{D_{kavg}}} \times \sqrt{\ln\left(\frac{s}{2r} + \sqrt{\left(\frac{s}{2r}\right)^2 - 1}\right)} \times \ln\left(\frac{W'+b}{w+t}\right)$$

$c$  = speed of light =  $2.99E+8$  m/s ( $1.18E+10$  in/s)

$s$  = via to via pitch

$r$  = radius of via barrel = Drill dia.

$\text{Stub\_len}$  = Total stub length

$$D_{kavg} = \frac{(D_{kxy} + D_{kz})}{2}$$

#### E. Circuit Model vs. HFSS Via Model Validation:

Using the HFSS model representing the actual test vehicle stack-up and long stub via pad/anti-pad stack,  $D_{keff}$  and  $Z_{via}$  were calculated using the parameters listed below. The dielectric constants were provided from supplier's data sheet [1] for the material used to fabricate the stack-up.

#### HFSS Via Parameters:

$s$  = 1.50 mm (59 mil)

$r$  = Drill radius = 0.36 mm (14 mil)

$\text{Via\_length}$  = 0.37 mm (14.7mil)

$\text{Stub\_length1}$  = 5.41 mm (212.9mil)

$\text{Stub\_length2}$  = 1.43 mm (56.3mil)

$\text{Stub\_length}$  = 6.84 mm (269.3mil)

Anisotropy in  $D_k$  = 18%

$W'$  = Anti-pad Length = 1.85 mm (73 mil)

$b$  = Oval anti-pad width = 1.35 mm (53 mil)

$B$  = Round anti-pad width = 1.68 mm (66 mil)

$w = t$  = Drill Diameter = 0.71mm (28 mil)

$$D_{kz} = 3.65$$

$$D_{kxy} = 1.18 \times 3.65 \cong 4.3$$

$$D_{kavg} = \left( \frac{3.65 + 4.3}{2} \right) = 3.96$$

#### Circuit Model Calculated Via Parameters:

$$D_{keff1} = D_{kavg} \times \frac{\ln\left(\frac{s}{2r} + \sqrt{\left(\frac{s}{2r}\right)^2 - 1}\right)}{\ln\left(\frac{W'+B}{w+t}\right)} = 6.00$$

$$D_{keff2} = D_{kavg} \times \frac{\ln\left(\frac{s}{2r} + \sqrt{\left(\frac{s}{2r}\right)^2 - 1}\right)}{\ln\left(\frac{W'+b}{w+t}\right)} = 6.73$$

$$TD_1 = \frac{\text{Stub\_len1}}{c} \times \sqrt{D_{keff1}} = 44.19 \text{ ps}$$

$$TD_2 = \frac{\text{Stub\_len2}}{c} \times \sqrt{D_{keff2}} = 12.38 \text{ ps}$$

$$f_0 = \frac{1}{4 \times TD} = \frac{1}{4 \times (TD_1 + TD_2)} = 4.42 \text{ GHz}$$

$$D_{keff} = \left[ \frac{c}{4 \times \text{Stub\_length} \times f_0} \right]^2 = 6.15$$

$$Z_{via\_Stub1} \cong \frac{60}{\sqrt{D_{kavg}}} \times \sqrt{\ln\left(\frac{s}{2r} + \sqrt{\left(\frac{s}{2r}\right)^2 - 1}\right)} \times \ln\left(\frac{W'+B}{w+t}\right) = 33.7 \Omega$$

$$Z_{via\_Stub2} \cong \frac{60}{\sqrt{D_{kavg}}} \times \sqrt{\ln\left(\frac{s}{2r} + \sqrt{\left(\frac{s}{2r}\right)^2 - 1}\right)} \times \ln\left(\frac{W'+b}{w+t}\right) = 31.8 \Omega$$

$$Z_{via} \cong \frac{(Z_{via\_Stub1} + Z_{via\_Stub2})}{2} = 32.8 \Omega$$

The simulated S-Parameters from the equivalent via circuit model were compared against the HFSS simulated touchstone S-parameter file using Agilent ADS [10]. Both circuit topologies used for the simulations are shown in Figure 9. Ideal Balun transformers were used to simplify the display of differential S-parameters. The common-signal properties were

not evaluated as they play no role in the behavior of the differential signal.

For such a simple model, the simulated insertion and return losses and phase of **Figure 10** to **Figure 12** respectively shows excellent correlation between these two computation methods up to approximately 13GHz. It is also remarkable the  $\frac{1}{4}$  resonant frequency calculated ( $f_0 = 4.42\text{GHz}$ ) agrees exactly to the simulated model.

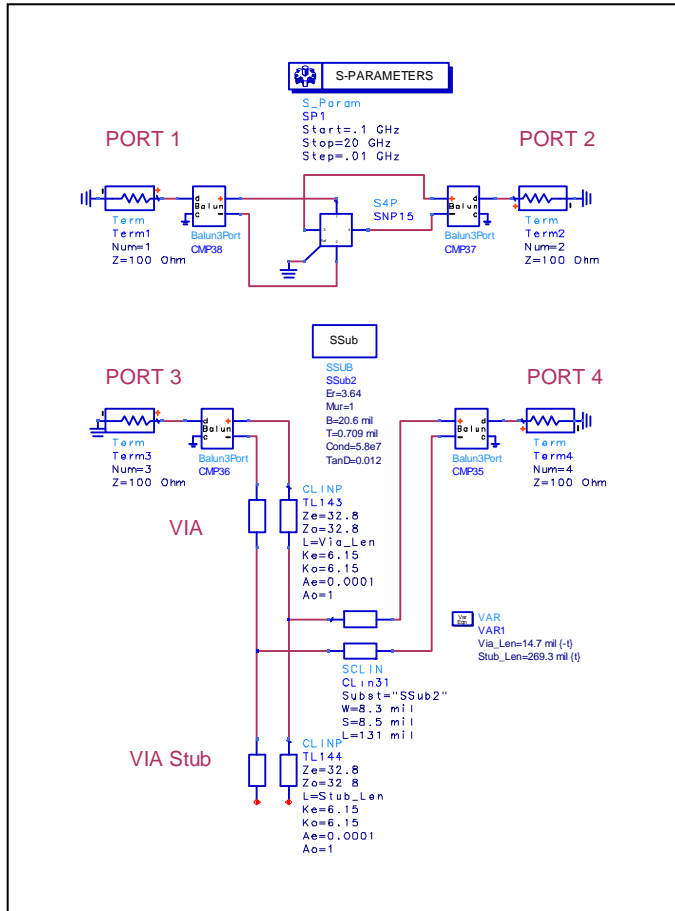


Figure 9 ADS schematic of HFSS touchstone S-parameter file ( $Dk_{xy} = 4.3$ ) (Ports 1, 2 top) vs. circuit model using calculated values (Ports 3, 4 bottom).

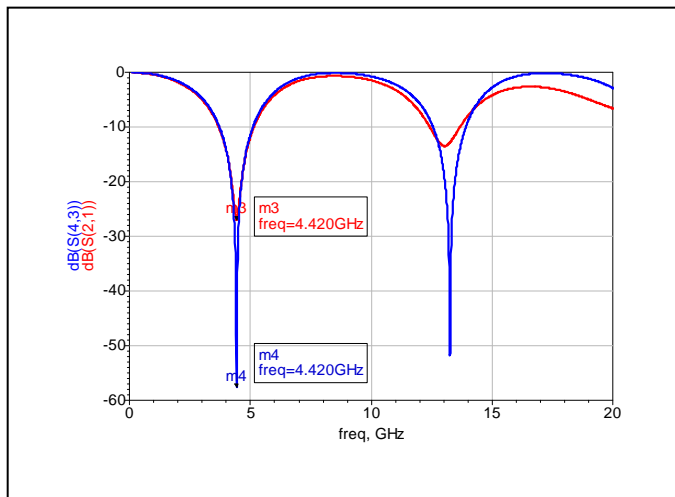


Figure 10 Simulated S(2,1) and S(4,3) Insertion Loss comparison of HFSS model (m3-red) against circuit model (m4-blue). The resonant frequency is 4.42GHz for both cases.

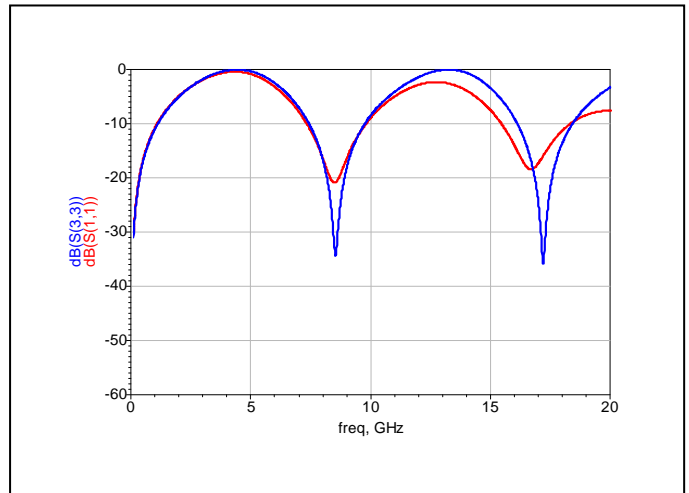


Figure 11 Simulated S(1,1) and S(3,3) Return Loss comparison of HFSS model (red) against circuit model (blue).

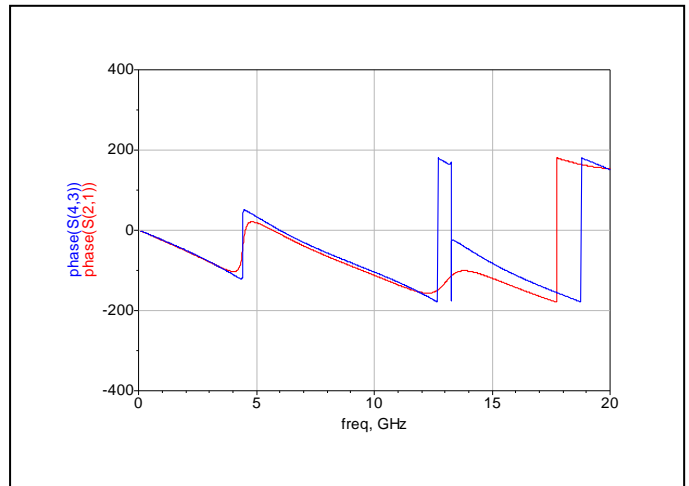


Figure 12 Simulated S(2,1) and S(4,3) Phase comparison of HFSS model (red) against circuit model (blue).

**F. Circuit Model vs. Test Vehicle Validation:**

Three different via structures representing long, medium and short differential via stubs as illustrated in **Figure 13** were chosen from the test vehicle [3], [5], [7]. The measured results were used to validate the differential via circuit model's accuracy.

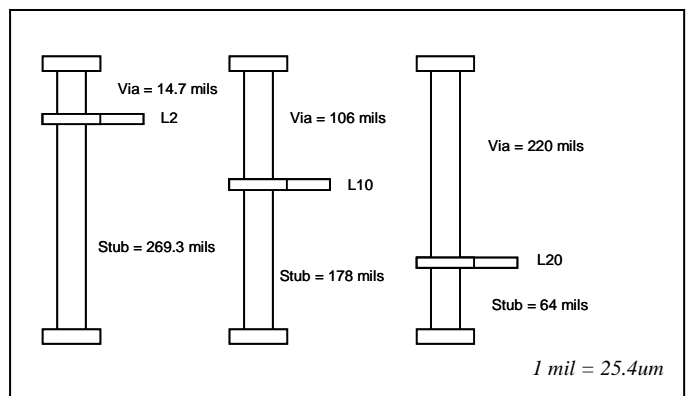


Figure 13 Illustration of layers measured showing long, medium, short stub lengths from test vehicle stack-up.



The test vehicle was set up and connected to an Agilent N5230A, 4 port 20 Gig Vector Network Analyzer (**Figure 14**) for each case. Two differential probes were fabricated from approximately 2 inch each of semi-rigid coax with SMA connectors terminating on one end. In order to facilitate probing the differential via hole structure, the other ends of the probes were stripped, and small length of solid wire was soldered to each semi-rigid coax sheath to provide a ground contact to adjacent ground reference holes. The probe tips were minimized in length to minimize loop inductance. The measurement setup was calibrated to the ends of the SMA cables using an Agilent E-Cal, module prior to connecting them to the custom probes. Since the semi-rigid probes were not part of the calibration, they are considered part of the device under test (D.U.T.) as outlined in the dashed rectangle (**Figure 14**).

Finally, a section of the coupon was cross-sectioned, and actual via to stub thickness ratios were measured for each stripline layer under a calibrated microscope.

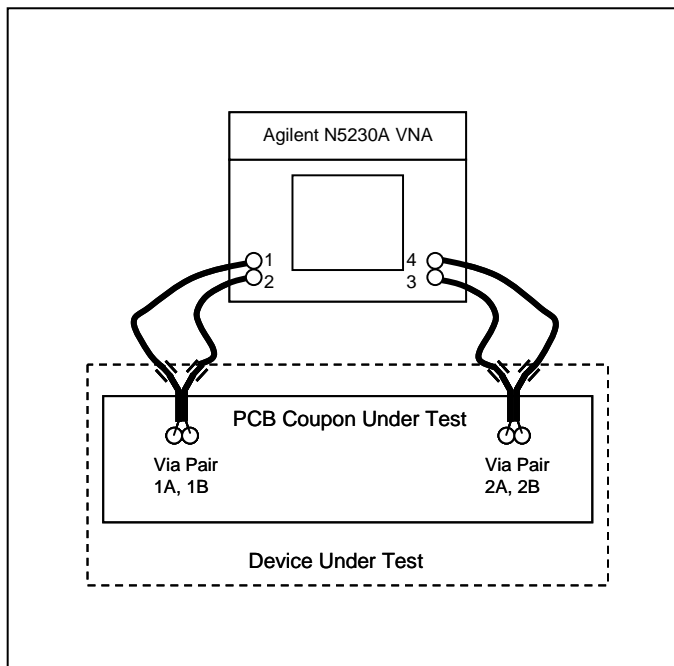


Figure 14 Test setup illustration. The test probes are considered part of the device under test.

The simulated S-parameters of the equivalent via circuit model for the long stub via case was compared against the HFSS generated touchstone S-parameter files and the measured results using Agilent ADS. The circuit topologies used for these simulations are shown in **Figure 15**.

The top circuit topology brings the measured S-parameters of the test vehicle into the simulation environment. The middle circuit topology brings the HFSS simulated S-parameter behavioral models for both vias and PCB traces. The bottom circuit topology simulated the transmission line elements using analytical formula parameters for the vias and traces. Ideal 4Port-Balun transformers realize the ideal transformation

between balanced (differential and common) signals and unbalanced (single-ended) signals. They were used to simplify the display of differential S-parameters and to terminate any differential to common mode conversion particularly with the measured data. For the medium and short stub cases, the respective circuit model was only compared to the measured results.

**Figure 16** shows the correlation of calculated results used in the circuit model against the measured test vehicle structure and HFSS model of the long stub via developed in [7]. The circuit simulation using the analytical calculations for the differential via  $D_{keff} = 6.15$  and odd-mode impedance of  $Z_{via} = 32.8 \Omega$  shows excellent agreement with the measurements to about 13 GHz. This also confirms the HFSS predictions of the via stub resonant frequency using the actual bulk dielectric constant of the laminate.

Updating  $D_{keff} = 6.25$  for medium stub case and 6.57 for short stub case to the respective via model, shows there is excellent agreement with measured results as seen in **Figure 17** and **Figure 18**. Furthermore, it is worth noting that the quarter-wave resonant frequency could not be measured from the test vehicle's measured data in the short stub case (**Figure 18**) because of the measurement bandwidth of 20GHz. This is a prime example to demonstrate the usefulness of the methodology presented in this paper to calculate  $D_{keff}$  rather than depend on measurements to calculate it.

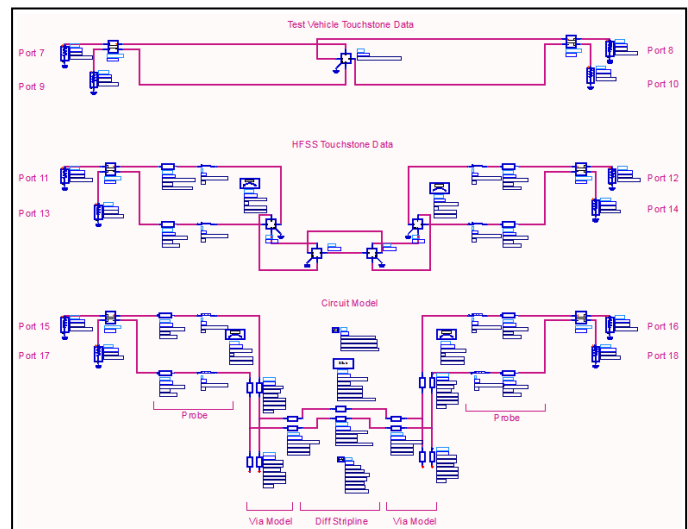


Figure 15 ADS schematic of test vehicle (top), HFSS (middle) and circuit model (bottom) used for simulation comparisons. The HFSS topology includes both via and track S-parameters as modeled from [7].

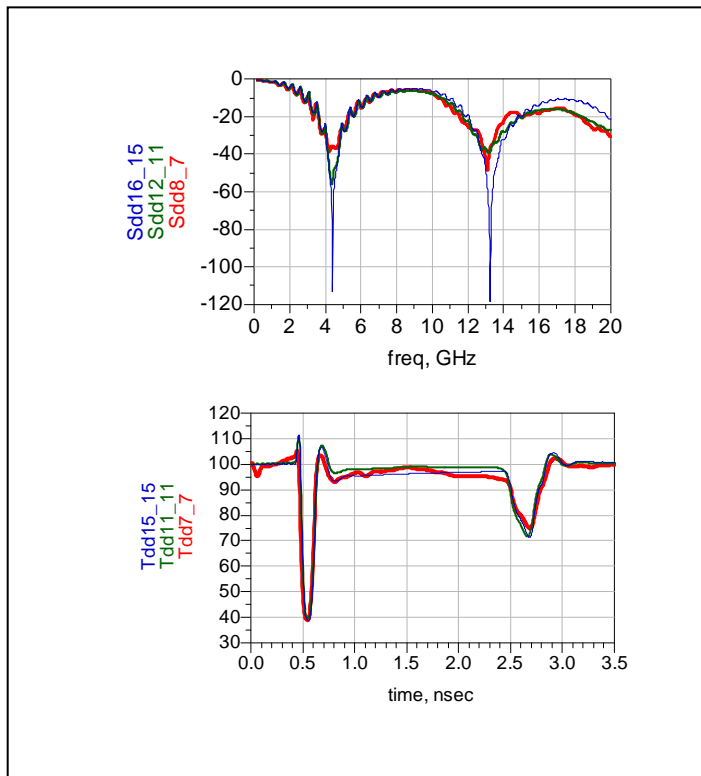


Figure 16 Long stub (L2) insertion loss (top) and TDR plots (bottom) comparison of test vehicle measurements (Sdd8\_7-red) against HFSS simulation (Sdd12\_11-green) and circuit model (Sdd16\_15-blue).  $D_{keff} = 6.15$ ,  $Z_{via} = 32.8$ ,  $D_f = 0.012$ .

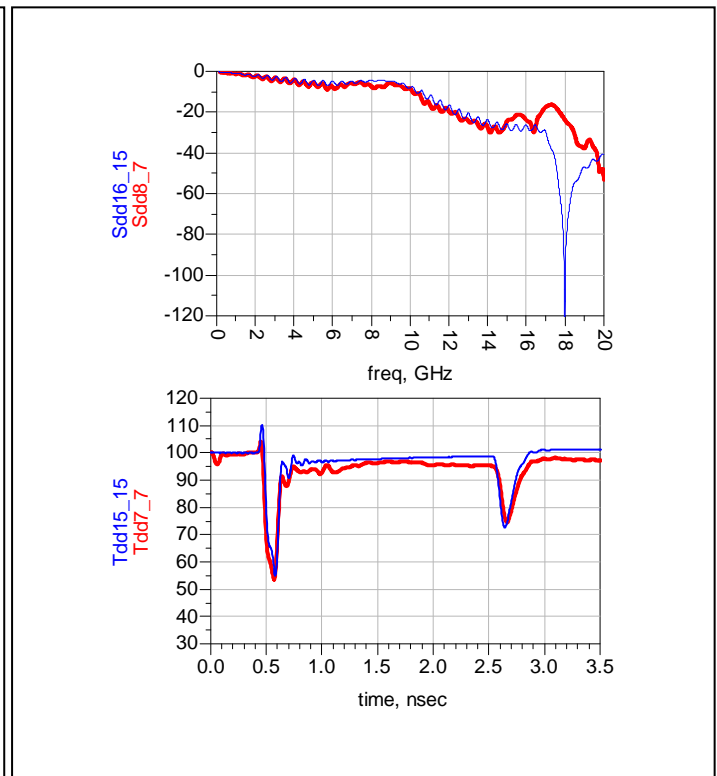


Figure 18 Short stub (L20) insertion loss (top) and TDR plots (bottom) comparison of test vehicle measurements (Sdd8\_7-red) against circuit model (Sdd16\_15-blue).  $D_{keff} = 6.57$ ,  $Z_{via} = 32.8$ ,  $D_f = 0.012$ .

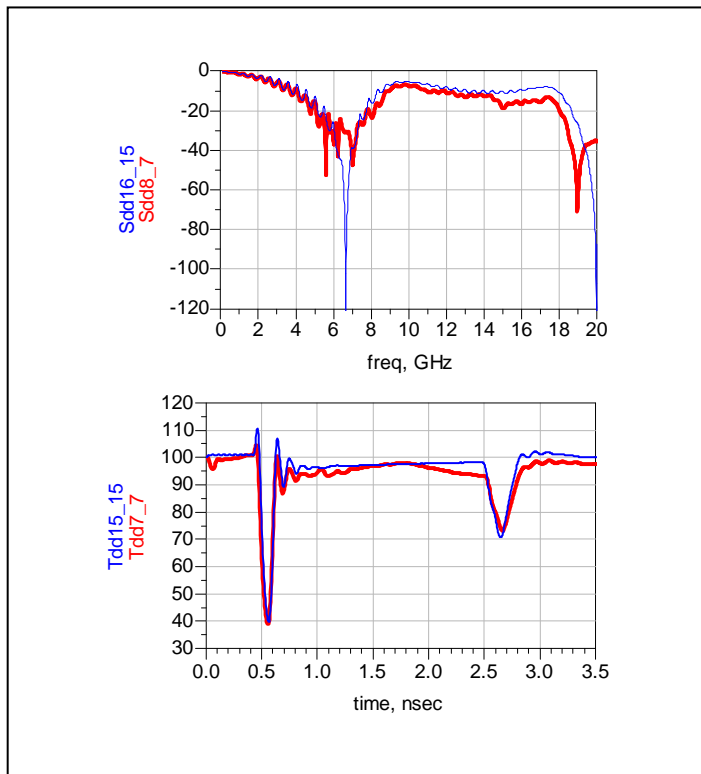


Figure 17 Medium stub (L10) insertion loss (top) and TDR plots (bottom) comparison of test vehicle measurements (Sdd8\_7-red) circuit model (Sdd16\_15-blue).  $D_{keff} = 6.25$ ,  $Z_{via} = 32.8$ ,  $D_f = 0.012$

#### IV. CONCLUSION

A novel equation based analytical methodology to develop a simple, scalable, high bandwidth circuit model of differential via holes has been introduced. The circuit model consisting of a pair of parameterized coupled transmission lines for both the through and stub portion of the via has shown it can be used to accurately describe a real differential via structure to very high bandwidth. Correlation to an EM-field solver and measured results suggests the model can be used as a first approximation to accurately describe a real differential via to very high bandwidth. In the absence of measured data or EM simulated results, applying this methodology can be used for sensitivity analysis to quickly quantify and optimize the performance of vias in a channel model or to help sanitize subsequent models generated with a 3D EM-field solver.

#### REFERENCES

- [1] Park Electrochemical Corp.
- [2] E. Bogatin, "Signal Integrity Simplified", Prentice Hall PTR, 2004.
- [3] L. Simonovich, "Relative Permittivity Variation Surrounding PCB Via Hole Structures," *Signal Propagation on Interconnects*, 2008, pp.1-4, May 2008.
- [4] P.I. Dankov, V.P. Levcheva, and V.N. Peshlov, "Utilization of 3D simulators for characterization of dielectric properties of anisotropic

materials," *Microwave Conference, 2005 European* , pp. 4-6, Oct. 2005

- [5] E. Bogatin, L. Simonovich, S. Gupta, M. Resso, "Practical Analysis of Backplane Vias", *DesignCon 2009*, Feb. 2009.
- [6] E. Bogatin, "Optimizing Vias for High Speed Serial Link Applications", *SI-Insights*, April, 2009.
- [7] Y. Cao, L. Simonovich, and Q.J. Zhang, "A wideband and parametric model of differential via holes using space-mapping neural network," *IEEE Microwave and Wireless Components Letters.*, vol. 19, pp. 533 - 535, Sep. 2009.
- [8] M.A.R. Gunston, "Microwave Transmission-Line Impedance Data", Van Nostrand Reinhold Company LTD. 1972.
- [9] *HFSS Version 11*, Ansoft Corporation, 2007.
- [10] *Agilent ADS*, Agilent EEs of EDA, 2009-Update 1.
- [11] L. Simonovich, E. Bogatin, Y. Cao, "Method of Modeling Differential Vias", White Paper, April 2009,



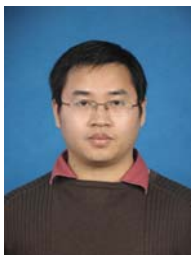
**Lambert Simonovich** (M'08) Born in Hamilton, Ontario, Canada, graduated in 1976 from Mohawk College of Applied Arts and Technology in Hamilton, Ontario, Canada as an Electronic Engineering Technologist. Over a 32 year career at Bell Northern Research and Nortel, he helped pioneer several advanced technology solutions into products and has held a variety of R&D positions, eventually specializing in backplane design over the last 25 years. He is the founder of Lamsim Enterprises Inc.

[www.lamsimenterprises.com](http://www.lamsimenterprises.com) providing innovative signal integrity and backplane solutions. He is currently engaged in signal integrity, characterization and modeling of high speed serial links associated with backplane interconnects. He holds two patents and (co)-author of several publications including an award winning DesignCon2009 paper related to via modeling.



**Eric Bogatin** received (M '80) his BS in physics from MIT and MS and PhD in physics from the University of Arizona in Tucson. He has held senior engineering and management positions at Bell Labs, Raychem, Sun Microsystems, Ansoft and Interconnect Devices. Eric has written 6 books on signal integrity and interconnect design and over 300 papers. His latest book, *Signal and Power Integrity- Simplified*, was published in 2009 by Prentice Hall. He has taught over 6,000 engineers in the last 20 years. Many of his papers and columns are posted on the

[www.BeTheSignal.com](http://www.BeTheSignal.com) web site.



**Yazhi Cao** (M'09) received the B.S. and Ph.D. degrees in electrical engineering from Wuhan University, Hubei, China, in 2004 and 2008, respectively. His research interests include neural network, design and modeling of RF/Microwave circuits.

Since 2009, he has been a postdoctor in the Department of Electronics, Carleton University, Ottawa, Canada.